Applied Physics Express **5** (2012) 032102
DOI: 10.1143/APEX.5.032102

Stable Circularly Polarized Emission from a Vertical-Cavity Surface-Emitting Laser with a Chiral Reflector

YiMing Zhu[1,2*], Fan Zhang[2*], GuanJun You[2], Jie Liu[2], John D. Zhang[1], Akhlesh Lakhtakia[2,3], and Jian Xu[1,2†]

[1]*Engineering Research Center of Optical Instrument and System, Ministry of Education, University of Shanghai for Science and Technology, No. 516 JunGong Road, Shanghai 200093, China*
[2]*Department of Engineering Science and Mechanics, Pennsylvania State University, University Park, PA 16802, U.S.A.*
[3]*Department of Physics, Indian Institute of Technology Kanpur, Kanpur 208016, India*

Received November 12, 2011; accepted January 29, 2012; published online February 27, 2012

An optically pumped vertical-cavity surface-emitting laser (VCSEL) was conceived, fabricated, and characterized for stable circularly polarized (CP) emission. This laser includes a columnar thin film as a quarter-wave plate and a chiral sculptured thin film as a chiral mirror for its microcavity. Pure CP lasing with a high degree of CP (~0.97) was observed when the VCSEL was optically pumped. The polarization of the laser output exhibits the same handedness as that of the chiral mirror.

Vertical-cavity surface-emitting lasers (VCSELs) with stable circularly polarized (CP) emission can be widely applied for biochemical sensing using circular dichroism (CD) and optical rotary dispersion,[1)] multispectral circular differential imaging,[2)] quantum computing and cryptography,[3)] polarized optical interconnects,[4)] and magnetic storage.[5)] There are, however, only a few reports on well-controlled CP emission from VCSELs except for studies on cholesteric-liquid-crystal resonators and on spin control of optically pumped VCSELs with CP output.[6–9)] Hence, much needs to be done in order to develop highly efficient VCSELs with well-controlled CP emission at room temperature.

We report here a novel approach to design and fabricate VCSELs with stable CP emission. A solid-state chiral sculptured thin film (CSTF) was used as a chiral mirror in the VCSEL configuration in order to control the polarization characteristics of the laser output, and thereby CP lasing was obtained upon optical pumping. At the pumping energy of 0.5 mJ, the degree of CP [defined as $(I_{\mathrm{RCP}} - I_{\mathrm{LCP}})/(I_{\mathrm{RCP}} + I_{\mathrm{LCP}})$, where $I_{\mathrm{RCP/LCP}}$ is the intensity of left/right CP emission] of the VCSEL emission was measured to be as high as ~0.97 at the lasing wavelength. This class of compactly packaged lasers can be fully integrated into optical/optoelectronic chips for several applications of CP light.

The chiral-mirror-based VCSEL is schematically illustrated in Fig. 1. The VCSEL design comprises, from the bottom up, a highly reflecting bottom distributed Bragg reflector (DBR) mirror, an n-type spacer layer, a gain layer of multiple quantum wells (MQWs), a p-type spacer layer, a partially reflecting top DBR mirror, a columnar thin film (CTF) functioning as an integrated quarter-wave plate (QWP), and a CSTF as a chiral mirror on the top.

A chiral mirror is an assembly of identical and parallel nanohelices with a diameter typically between 10 and 100 nm. Upon excitation by light with the wave vector aligned parallel to the nanohelices, a CSTF displays the circular Bragg phenomenon in a narrow wavelength range (Bragg regime): incident CP light of the same handedness as the CSTF is highly reflected, while incident CP light of different handedness is reflected very little. This property arises from the interaction of the local linear birefringence with the structural chirality. For design purposes, the Jones matrix representation of a chiral mirror has been derived from its CP-selective transmission and reflection properties for normal incidence. For incident cohanded CP light, the Jones matrix of a structurally left-handed chiral mirror is $T_{\mathrm{CSTF}}^{\mathrm{Left}} = (1 - R - S)/2\begin{bmatrix} 1 & -i \\ -i & -1 \end{bmatrix}$, and that of a structurally right-handed chiral mirror is $T_{\mathrm{CSTF}}^{\mathrm{Right}} = (1 - R - S)/2\begin{bmatrix} 1 & i \\ i & -1 \end{bmatrix}$, where R is the intensity reflection coefficient (reflectance), and S is the scattering loss of light propagating through the chiral mirror.

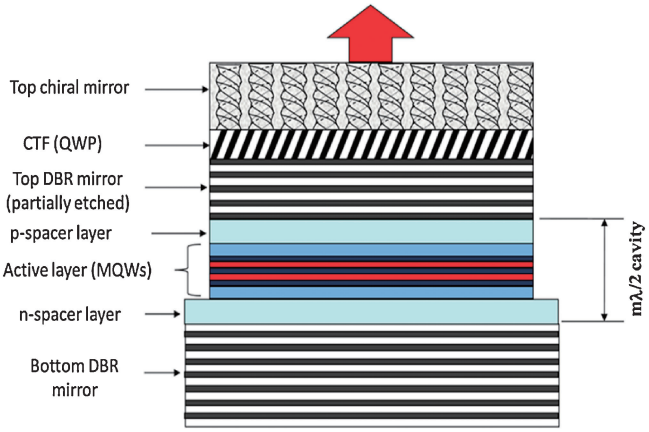

Fig. 1. Schematic of a VCSEL that contains a CTF and a CSTF.

The microstructure of the CTF (QWP component of the VCSEL) is similar to that of the CSTF except that the nanohelices are replaced by nanorods with anisotropic cross-sectional morphology.[12)] A CTF exhibits linear birefringence with the fast axis defined in the deposition plane. The phase retardance of a CTF is proportional to its birefringence and its thickness, both of which were tailored for the integrated QWP in the present study.[12)]

The integrated QWP breaks the otherwise rotational symmetry of the VCSEL configured with a chiral mirror by introducing a fast axis in the transverse plane. Two orthogonally polarized modes, characteristic of spatial variations inside the cavity, are present for the VCSEL, each of which is composed of a linearly polarized state between the bottom and top DBR reflectors and a CP state between the top DBR mirror and chiral mirror. For the first mode, the linearly polarized electric field makes an angle of

*These two authors contributed equally to this work.
†E-mail address: Jianxu@engr.psu.edu

+45° with the fast axis of the QWP, which converts the linearly polarized light into left circularly polarized (LCP) light. For the second mode, the linearly polarized electric field makes an angle of −45° with the fast axis of the QWP, which converts it into right circularly polarized (RCP) light. If the structural handedness of the chiral mirror is the same as that of the CP light, light will be reflected with low return loss and become resonant in the cavity toward the onset of stimulated emission of one of the two modes. In contrast, CP light of different handedness (for the other mode) will be largely transmitted by the chiral mirror, which results in high cavity losses. It's worth pointing out that the presence of the partially reflecting top DBR in the current VCSEL design helps to suppress the return losses in the cavity because reflection from a chiral mirror is often accompanied by loss due to the multiple scattering from the nanohelices.

This analysis is supported by the eigenstates of the electric field in front of the chiral mirror of VCSEL from the overall Jones matrix M for one round trip inside the VCSEL cavity. Specializing for a structurally right-handed chiral mirror for definiteness, we get

$$\begin{aligned} M &= \sqrt{R_{\mathrm{DBR}} R_{\mathrm{CSTF}}}\, G_{\mathrm{linear}} \\ &\quad \times \exp(2ikL) T_{\mathrm{QWP}} T_{\mathrm{coordinate}} T_{\mathrm{QWP}} T_{\mathrm{coordinate}} T_{\mathrm{CSTF}}^{\mathrm{Right}} \\ &= \sqrt{R_{\mathrm{DBR}} R_{\mathrm{CSTF}}}\, G_{\mathrm{linear}} \exp(2ikL) \begin{bmatrix} 1 & i \\ i & 1 \end{bmatrix}, \end{aligned} \tag{1}$$

where k is the wavenumber of the intracavity field, R_{DBR} is the reflectance of the bottom DBR, R_{CSTF} is the reflectance of the chiral mirror for cohanded CP incident light, G_{linear} is the double-pass complex gain associated with linear polarization in the gain layer of MQWs, TQWP is the Jones matrix of the QWP, and $T_{\mathrm{coordinate}}$ is a coordinate-transformation matrix.[10)]

The matrix M of eq. (1) has two eigenvectors, one LCP and the other RCP. Only the RCP eigenvector has a nonzero eigenvalue, suggesting that the RCP mode is the only contained mode in the VCSEL. It is worth mentioning that, as the reflection of CP light from conventional mirrors (such as metal mirrors and DBR mirrors) invariably inverts the handedness, a chiral mirror cannot be replaced in our VCSEL by a conventional mirror.

Device fabrication started from epitaxial growth of a conventional VCSEL over a (001) GaAs substrate by metal organic chemical vapor deposition (MOCVD). The bottom DBR mirror consists of 34 pairs of $Al_{0.9}Ga_{0.1}As/Al_{0.12}Ga_{0.88}As$ with ≥99.9% reflectance at the design wavelength ($\lambda \sim 850$ nm). The $3\lambda/2$-thick undoped active region consists of two $Al_{0.3}Ga_{0.7}As/GaAs/Al_{0.3}Ga_{0.7}As$ quantum wells placed at the antinode positions of the standing wave. The top DBR mirror has 22 unit cells of $Al_{0.9}Ga_{0.1}As/Al_{0.12}Ga_{0.88}As$. The DBR mirrors of the VCSEL exhibit a well-defined Bragg regime centered at $\lambda = 850$ nm with an full width at half maximum (FWHM) linewidth of 74 nm.

Next, the top DBR mirror of the VCSEL was precisely thinned down to ∼18 pairs by a wet etching process involving phosphoric acid ($H_3PO_4 : H_2O_2 : H_2O = 1 : 1 : 100$). This led to reduced reflectance (∼75%) in the top DBR layer, and paved the way for introducing the combination of a QWP and a chiral mirror for CP-selective feedback in the VCSEL. Sequential deposition of a CTF and a CSTF over the thinned top DBR was performed in an e-beam evaporator using the serial bideposition (SBD) technique.[11,12)] At the top of the cross-sectional scanning electron microscopy (SEM) image of the fabricated VCSEL in Fig. 2, the structurally right-handed chiral mirror of 4.157 μm thickness contains eight-period nanohelices. The CTF below the CSTF has a thickness of 1.449 μm. To fabricate both the CTF and the CSTF, TiO_2 was chosen because of its high bulk refractive index (= 2.6) and excellent optical transparency at the lasing wavelength. A cross-sectional SEM image of a fabricated VCSEL is provided in Fig. 2, wherein the chiral mirror is structurally right-handed.

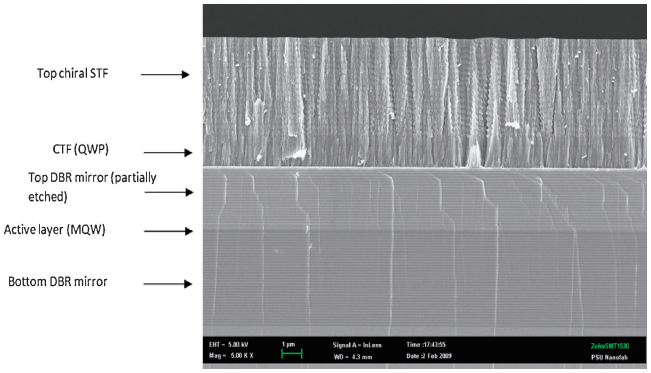

Fig. 2. Cross-sectional scanning electron microscopy image of a fabricated VCSEL containing a bottom DBR mirror (with 34 unit cells), a $3\lambda/2$ inner cavity, two quantum wells, a top DBR mirror (with 18 unit cells), a CTF acting as a QWP, and a structurally right-handed CSTF acting as a chiral mirror. The contact layers are too thin to be identified in this micrograph.

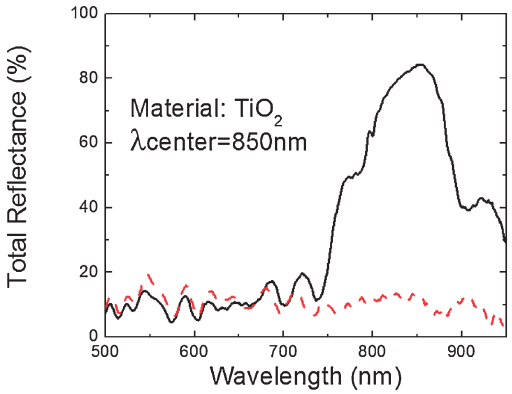

Fig. 3. Measured reflectance spectra of the CTF+CSTF combination. The incident electric field vector is oriented either at +45° (black solid line) or −45° (red dashed line) with respect to the fast axis of the CTF. The CSTF is structurally right-handed.

Figure 3 shows the normal-incidence reflectance spectra of the CTF+CSTF combination measured for incident light of two different linear polarization states: the incident electric field vector is oriented at ±45° with respect to the fast axis of the QWP. A Bragg regime is distinctively observed for the +45° orientation, which translates to RCP reflection upon light propagation through the QWP, whereas insignificant reflection of the −45° orientation, which

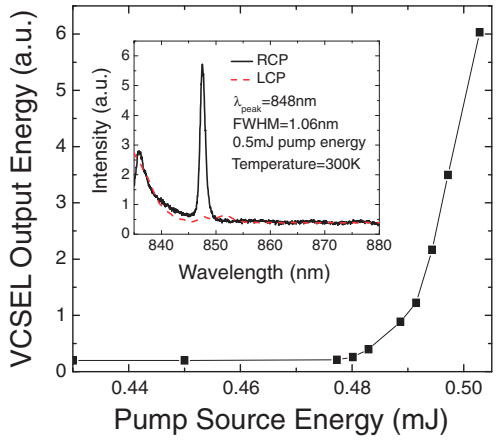

Fig. 4. VCSEL output energy versus pumping energy at room temperature. The inset is the spectrum of the RCP laser emission at the pumping source energy of 0.5 mJ. The spectrum of LCP emission is also included for comparison.

translates to LCP reflection upon light propagation through QWP, was measured due to the CP selectivity of the chiral mirror. The center wavelength of the Bragg regime of the chiral mirror is ~850 nm, which had been designed to match the lasing wavelength of the VCSEL. The FWHM bandwidth is ~65 nm. The peak reflectance in the Bragg regime was measured as 84%.

For lasing characterization, the VCSEL configured with the CTF+CSTF combination was pumped with femtosecond laser pulse with central wavelength at 800 nm, which was produced by a femtosecond amplifier (Libra, Coherent Inc., 70 fs pulse duration, 1 kHz repetition rate, 1 mJ pulse energy, horizontal linear-polarization). The incident angle of pump beam is ~45 degree, and the beam diameter at the incident surface is ~2 mm. A dichroic lens was used to couple the pump laser into the VCSEL and transmit the output signal. After passing through a longpass filter, which further screened out the laser light at the pumping wavelength, the VCSEL output was divided into two parts by a beam splitter: one part was delivered to a spectrometer (SP-2500i, ACTON Inc., 0.1 nm wavelength resolution) for spectral analysis, while the other was sent down to an optical bench comprising a quarter-wave Fresnel-rhomb retarder, a Glan–Thompson prism analyzer, and a low-power detector to characterize the CP purity of the VCSEL output. The Fresnel-rhomb retarder converts CP light to linearly polarized light over the wavelength range of interest. The degree of CP of the emission was characterized by measuring the analyzer transmission as a function of the optical-axis orientation of the analyzer.

Figure 4 plots the polarization-independent measurement result of the VCSEL output as a function of the pump fluence, which shows a typical threshold behavior for lasing action. A threshold energy of ~0.49 mJ was observed at room temperature, beyond which the VCSEL emission increases drastically. At the pumping energy of 0.5 mJ, the polarization-resolved lasing spectra shown in the inset of Fig. 4 were recorded. A sharp peak at $\lambda = 848$ nm was measured for the RCP emission, exhibiting a single longitudinal lasing mode. The corresponding FWHM linewidth is ~1.06 nm. The $3\lambda/2$ cavity design accounts for the observed single-mode laser operation. The spectrum of LCP light was also measured under the same operational conditions and plotted for the sake of comparison. The degree of CP is ~0.97 at peak lasing wavelength. The results clearly indicate that RCP oscillation dominates in the VCSEL, while the LCP oscillation is highly suppressed and cannot yield pronounced lasing output. At higher pump power, it was also found that the degree of polarization of the laser output remains approximately the same.

It is noteworthy that the observed CP lasing behavior is fundamentally different from employing CP filters in front of a conventional VCSEL: The presence of a right-handed chiral mirror in front of a conventional VCSEL will block RCP emission and transmit the LCP component of the laser output, which differs completely from the observed RCP emission characteristic of the present VCSEL design.

In summary, a conventional VCSEL integrated with a quarter wave plate and a chiral mirror, both grown as sculptured thin films, was conceived and designed to realize CP emission. Measurements of the CP resolved intensity and threshold behavior of the VCSEL output have suggested that the only self-contained mode in the microcavity is the CP oscillation with the same handedness as the structural handedness of the chiral mirror. Pure CP lasing with the same handedness as that of the chiral mirror was observed by the external optical pumping method.

Acknowledgments The work at University of Shanghai for Science and Technology was supported by Science and Technology Commission of Shanghai under grants 11530502200 and 1052nm07100, Ministry of Education Doctoral Fund for new teachers of China under grant 20093120120007, Ministry of Education Scientific Research Foundation for Returned, the National Natural Science Foundation of China under grant 61007059, Program for New Century Excellent Talents in University and NSFC under grant 61078007. The work at the Penn State University is being supported by the National Science Foundation under grants CMMI-0729263 and ECCS 0824186, and the Charles Godfrey Binder Endowment at Penn State.

1) T. I. Karu, S. F. Kolyakov, L. V. Pyatibrat, E. L. Mikhailov, and O. N. Kompanets: Proc. SPIE **4433** (2001) 97.
2) T. W. King, G. L. Coté, R. McNichols, and M. J. Goetz, Jr.: Opt. Eng. **33** (1994) 2746.
3) E. Pazy, T. Calarco, I. D'Amico, P. Zanardi, F. Rossi, and P. Zoller: J. Supercond. **16** (2003) 383.
4) P. Bhattacharya: *Semiconductor Optoelectronic Devices* (Prentice Hall, New York, 1996).
5) C. D. Stanciu, F. Hansteen, A. V. Kimel, A. Kirilyuk, A. Tsukamoto, A. Itoh, and Th. Rasing: Phys. Rev. Lett. **99** (2007) 047601.
6) Y. Tanaka, H. Takano, and T. Kurokawa: Jpn. J. Appl. Phys. **43** (2004) 1062.
7) S. Hovel, N. Gerhardt, M. Hofmann, J. Yang, D. Reuter, and A. Wieck: Electron. Lett. **41** (2005) 251.
8) H. Ando, T. Sogawa, and H. Gotoh: Appl. Phys. Lett. **73** (1998) 566.
9) S. Iba, S. Koh, K. Ikeda, and H. Kawaguchi: Appl. Phys. Lett. **98** (2011) 081113.
10) F. Zhang, J. Xu, A. Lakhtakia, T. Zhu, S. M. Pursel, and M. W. Horn: Appl. Phys. Lett. **92** (2008) 111109.
11) I. J. Hodgkinson and Q. H. Wu: Appl. Opt. **38** (1999) 3621.
12) I. J. Hodgkinson, Q. H. Wu, B. Knight, A. Lakhtakia, and K. Robbie: Appl. Opt. **39** (2000) 642.